Science Advances

AAAS

advances.sciencemag.org/cgi/content/full/2/8/e1600480/DC1

Supplementary Materials for

Mechanized azobenzene-functionalized zirconium metal-organic framework for on-command cargo release

Xiangshi Meng, Bo Gui, Daqiang Yuan, Matthias Zeller, Cheng Wang

Published 3 August 2016, *Sci. Adv.* **2**, e1600480 (2016)
DOI: 10.1126/sciadv.1600480

This PDF file includes:

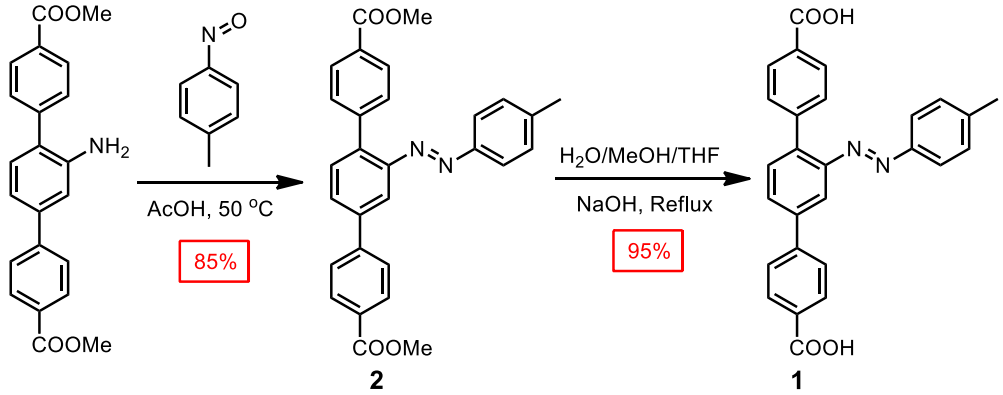

fig. S1. Synthesis of ligand 1.

Synthesis of compound 2: The mixture of *p*-nitrosotoluene (3.02 g, 24.9 mmol) and dimethyl 2′-amino-1,1′:4,1″-terphenyl-4,4″-dicarboxylate (2.03 g, 5.62 mmol) in acetic acid (200 mL) was stirred and heated at 50 ºC for 3 days under N_2 atmosphere. The reaction mixture was cooled down to room temperature and then neutralized with saturated $NaHCO_3$ solution. The solution was then extracted with ethyl acetate (100 mL × 3), and the combined extracts was washed with brine and dried over Na_2SO_4. After that, the solvents were evaporated under reduced pressure and the resulting residue was subjected to column chromatography [SiO_2 : CH_2Cl_2 / petroleum ether (1 : 1)] and compound **2** was isolated as orange solid (2.21 g, 85%, yield). ^{1}H NMR (400 MHz, $CDCl_3$, ppm): δ = 8.17 – 8.11 (m, 4H), 8.03 (d, J = 1.9 Hz, 1H), 7.84 – 7.81 (m, 3H), 7.73 – 7.68 (m, 3H), 7.61 – 7.58 (m, 2H), 7.28 (d, J = 8.1 Hz, 2H), 3.97 (s, 3H), 3.96 (s, 3H), 2.43 (s, 3H). ^{13}C NMR (75 MHz, $CDCl_3$, ppm): δ = 167.2, 151.0, 150.0, 144.5, 143.2, 142.2, 140.5, 139.5, 131.4, 130.9, 130.3, 130.0, 129.5, 129.2, 129.0, 127.2, 123.5, 114.8, 52.3, 21.7. HR-MS (ESI): calcd for $C_{29}H_{24}N_2O_4$: 464.1736 $[M]^+$; found, 464.1741 $[M]^+$.

Synthesis of ligand 1: In a mixture of 20% NaOH aqueous solution (40 mL), MeOH (40 mL) and THF (40 mL), compound **2** (2.09 g, 4.50 mmol) were added. The reaction mixture was refluxed for 12 h. After cooling to room temperature, MeOH and THF were evaporated under reduced pressure. Additional water (40 mL) was added and the mixture was heated until the solid was fully dissolved, then the solution was acidified with diluted HCl until no further precipitate was detected (PH ≈ 2). The precipitate was collected by filtration, washing with water and drying in vacuum. Ligand **1** was isolated as orange solid (1.86 g, 95%, yield). ^{1}H NMR (300 MHz, DMSO-d_6, ppm): δ = 13.11 (s, 2H), 8.09 – 8.00 (m, 6H), 7.94 (d, J = 8.2 Hz, 2H), 7.83 (d, J = 8.0 Hz, 1H), 7.67 (m 4H), 7.39 (d, J = 8.0 Hz, 2H), 2.39 (s, 3H). ^{13}C NMR (100 MHz, DMSO-d_6, ppm): δ = 167.3, 167.1, 150.4, 149.4, 142.2, 139.7, 138.9, 130.9, 130.3, 130.2, 130.1, 129.8, 129.5, 128.9, 127.1, 123.0, 114.0, 21.1.

HR-MS (ESI): calcd for $C_{27}H_{19}N_2O_4$: 435.1345 $[M-H]^-$; found, 435.1345 $[M-H]^-$.

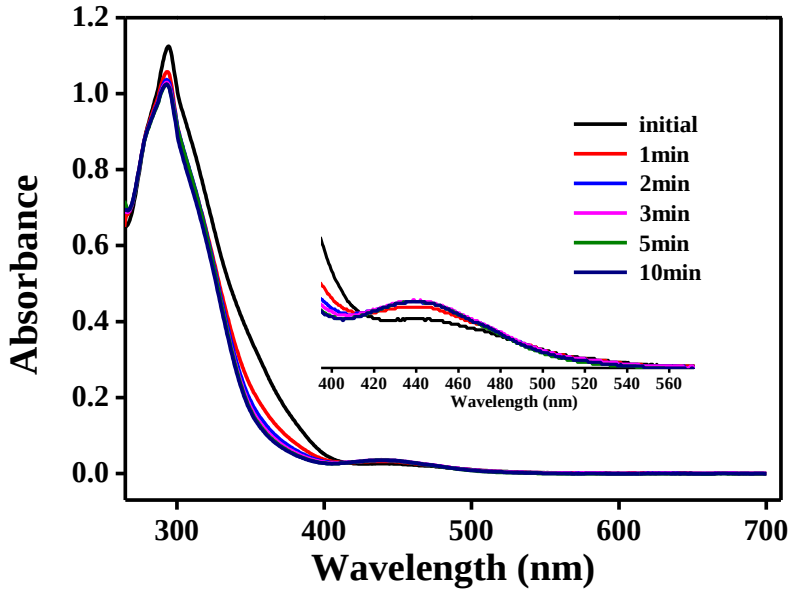

fig. S2. UV-visible spectra of ligand 1 after exposure to UV light (365 nm) for different times.

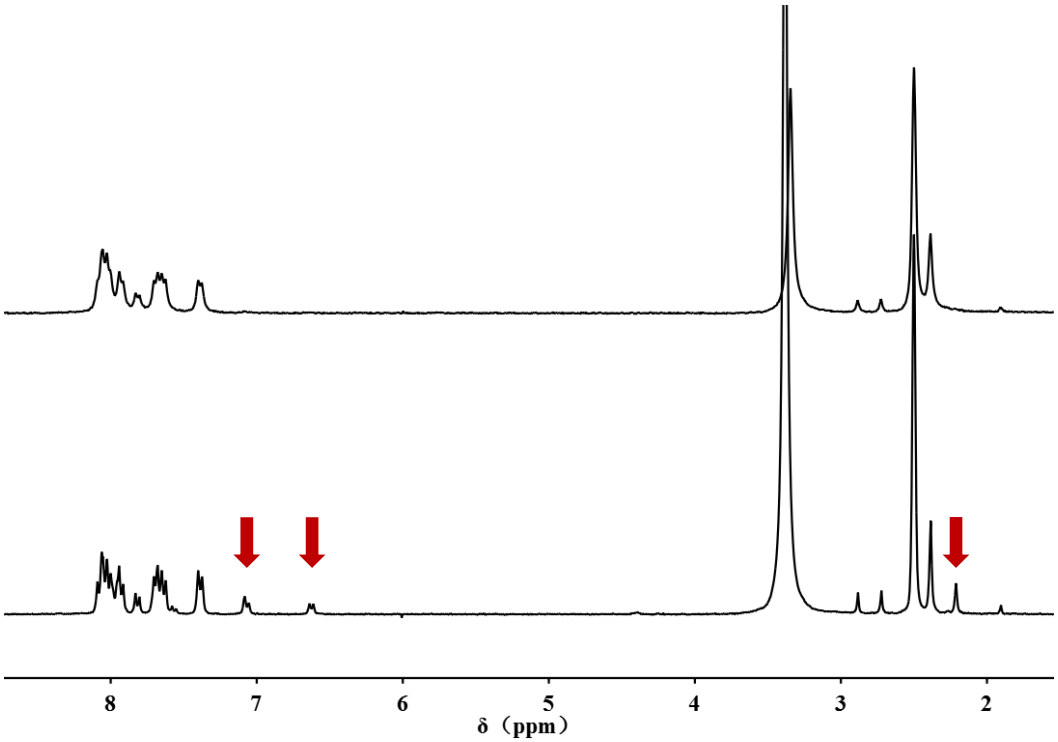

fig. S3. ^{1}H NMR (300 MHz, DMSO-d_6) spectrum of ligand 1 (up) and ligand 1 (down) after UV (λ = 365 nm) irradiation for 5 min. Red arrows indicate the new peaks from *cis* isomer after UV irradiation.

table S1. Crystal data and structure refinement for UiO-68-azo.

Identification code	UiO-68-azo
CCDC No.	1448512
Empirical formula	C_{162} H_{105} $N_{12}O_{32}$ Zr_6
Formula weight	3278.89
Temperature	100(2) K
Wavelength	0.800 Å
Crystal system	Cubic
Space group	$Fm\bar{3}m$
Unit cell dimensions	a = 32.7875(12) Å, α= 90°
	b = 32.7875(12) Å, β = 90°
	c = 32.7875(12) Å, γ = 90°
Volume	35247(4) $Å^3$
Z	4
Density (calculated)	0.618 Mg/m^3
Absorption coefficient	0.282 mm^{-1}
F(000)	6628
Crystal size	0.230 × 0.220 × 0.170 mm^3
Theta range for data collection	2.422 to 29.796°.
Index ranges	-40<=h<=40, -27<=k<=40, -28<=l<=40
Reflections collected	30077
Independent reflections	1789 [R(int) = 0.0622]
Completeness to theta = 28.685°	99.7 %
Absorption correction	None
Refinement method	Full-matrix least-squares on F^2
Data / restraints / parameters	1789 / 54 / 54
Goodness-of-fit on F^2	1.077
Final R indices [I>2σ(I)]	R_1 = 0.0504, wR_2 = 0.1406
R indices (all data)	R_1 = 0.0626, wR_2 = 0.1494
Extinction coefficient	0.00037(6)

Largest diff. peak and hole	0.628 and -1.092 e.Å^{-3}

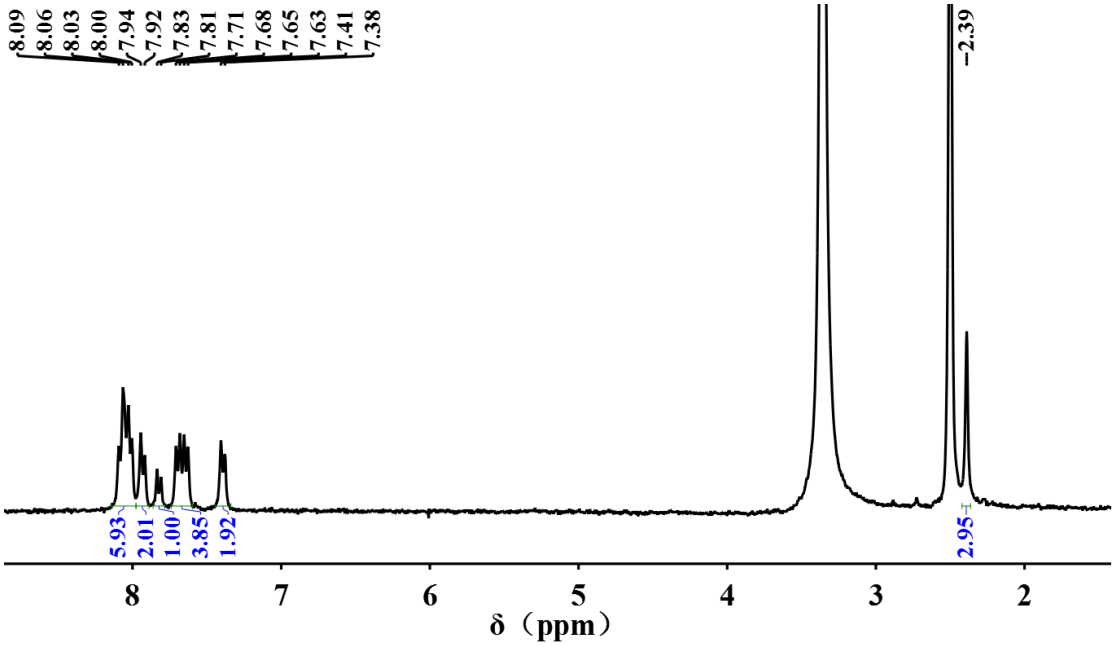

fig. S4. ^{1}H NMR (300 MHz, DMSO-d_6) spectrum of digested UiO-68-azo.

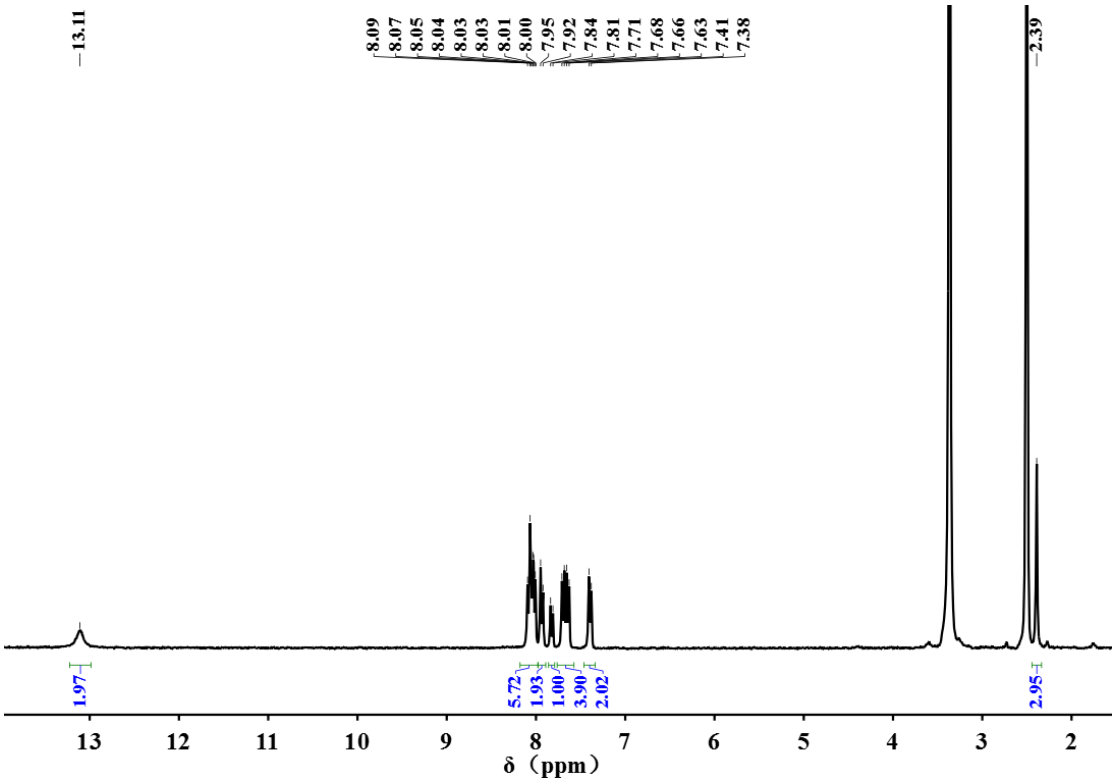

fig. S5. ^{1}H NMR (300 MHz, DMSO-d_6) spectrum of ligand 1.

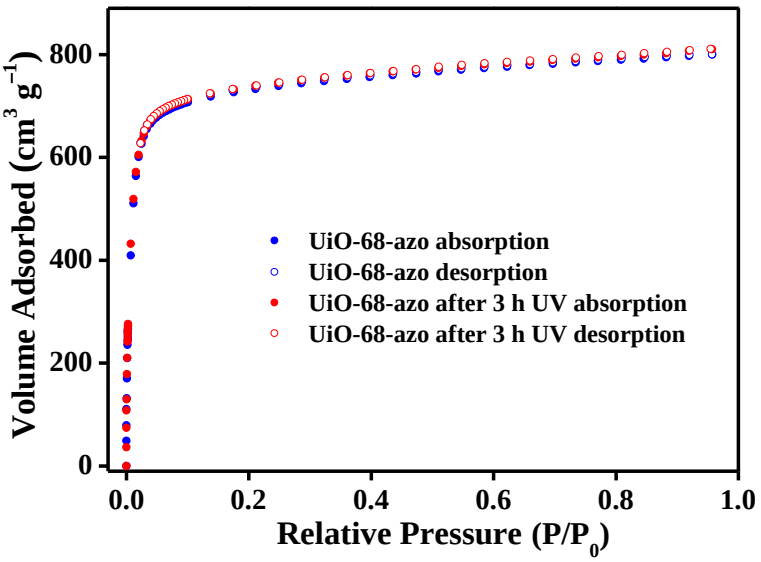

fig. S6. N_2 sorption isotherm of UiO-68-azo at 77 K before and after UV irradiation for 3 hours.

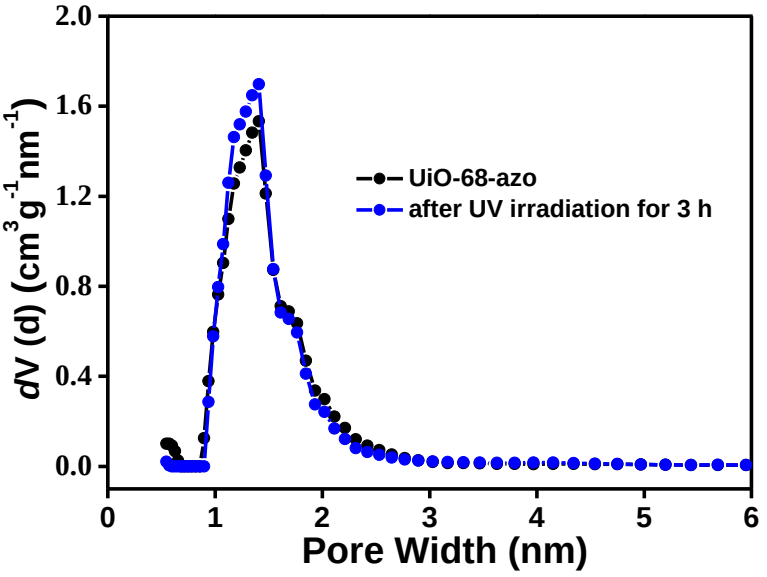

fig. S7. Pore size distribution of UiO-68-azo before and after UV irradiation for 3 hours.

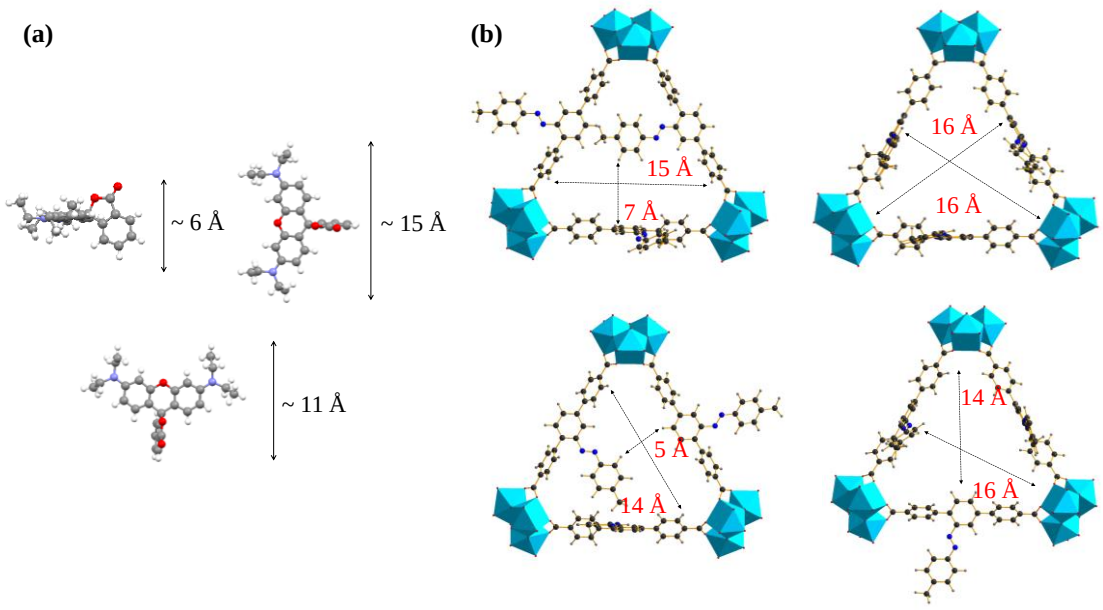

fig. S8. Size comparison of RhB and the pore windows of UiO-68-azo. (**a**) RhB size without counterion in three dimensions. (**b**) the size of some triangle windows in UiO-68-azo.

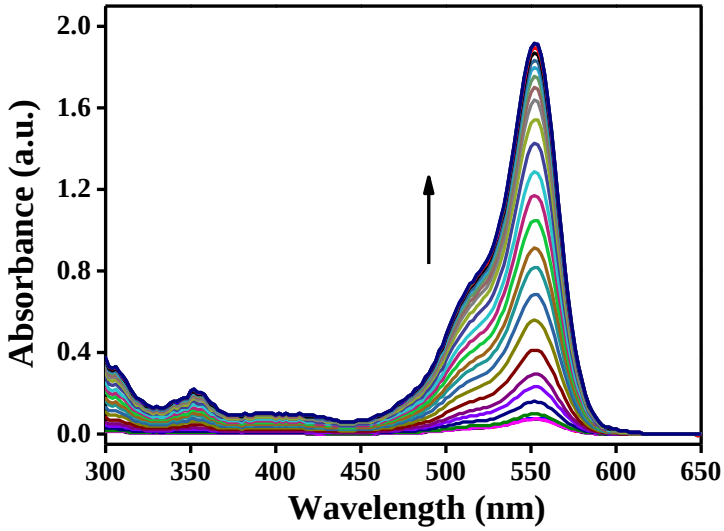

fig. S9. UV-visible spectra of the solution after UV irradiation for different time. Condition: ~8.6 mg UiO-68-azo, 25 mL deionized water.

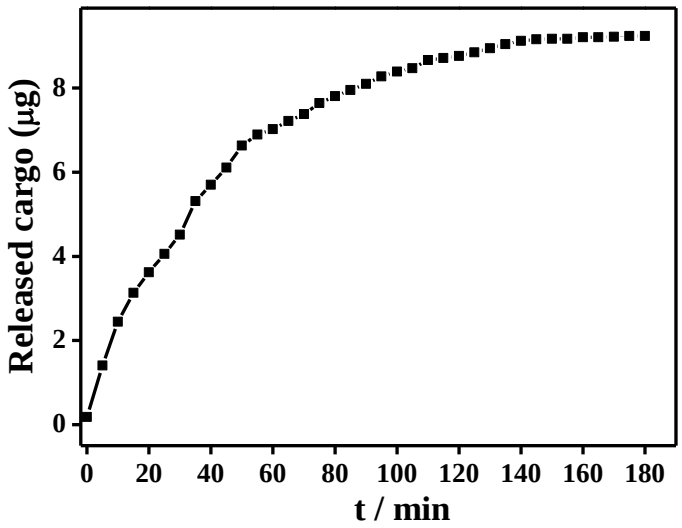

fig. S10. Release profile of uncapped RhB-loaded UiO-68-azo. The RhB can be spontaneously released from the nanopores of UiO-68-azo, confirming that UiO-68-azo with no *pseudo*-rotaxanes on the surface cannot store a cargo of RhB. Condition: ~2.5 mg UiO-68-azo, 3 mL deionized water.

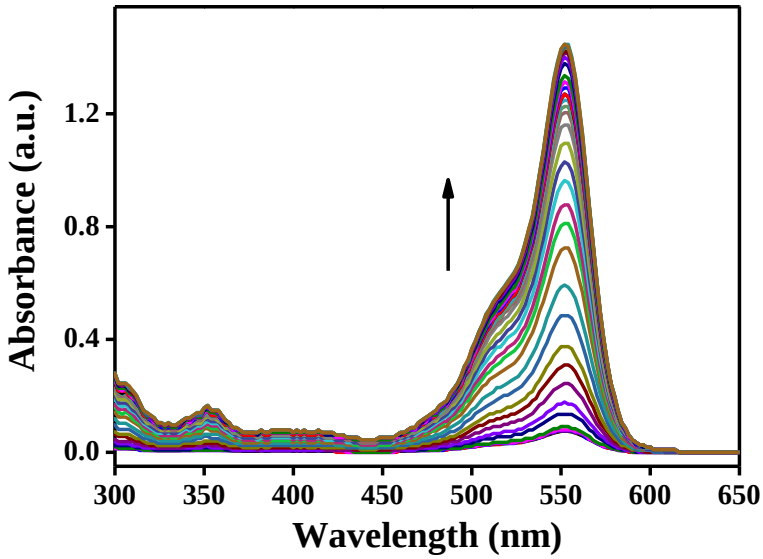

fig. S11. UV-visible spectra of the solution after addition of amantadine and then UV irradiation for different time. Condition: ~6.3 mg UiO-68-azo, 25 mL deionized water, 2 mg amantadine.

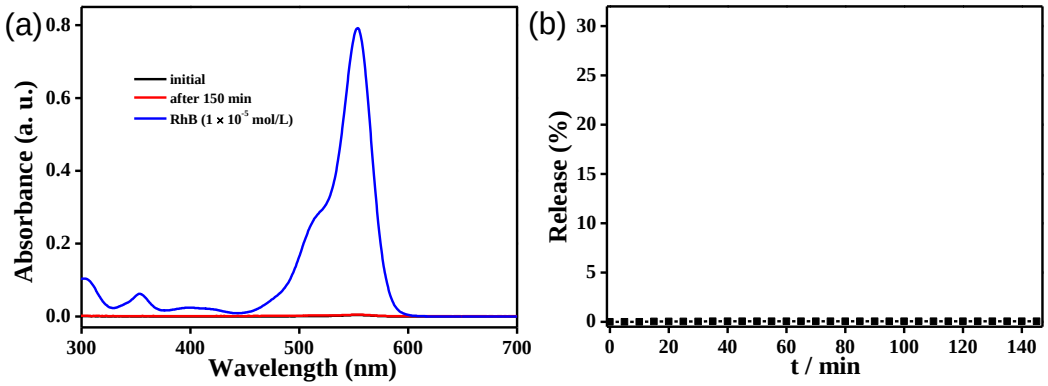

fig. S12. UV spectra (**a**) and release profile (**b**) of mechanized UiO-68-azo after addition of D-arabinose. Condition: ~3.2 mg UiO-68-azo, 3 mL deionized water, 1 mg D-arabinose.

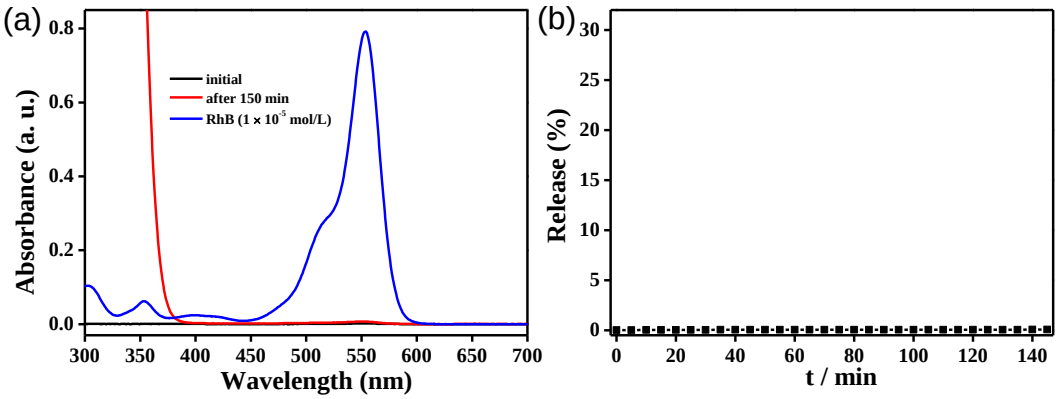

fig. S13. UV spectra (**a**) and release profile (**b**) of mechanized UiO-68-azo after addition of 4-amino-1-naphthalenesulfonic acid sodium salt. The absorption below 375 nm (red line) should be ascribed to the additive. Condition: ~3.3 mg UiO-68-azo, 3 mL deionized water, 1 mg 4-amino-1-naphthalenesulfonic acid sodium salt.

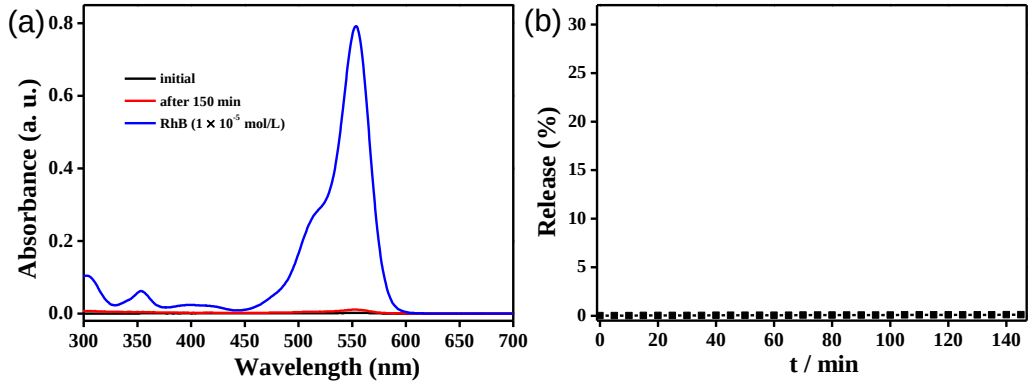

fig. S14. UV spectra (**a**) and release profile (**b**) of mechanized UiO-68-azo after addition of sodium benzoate. Condition: ~3.6 mg UiO-68-azo, 3 mL deionized water, 1 mg sodium benzoate.

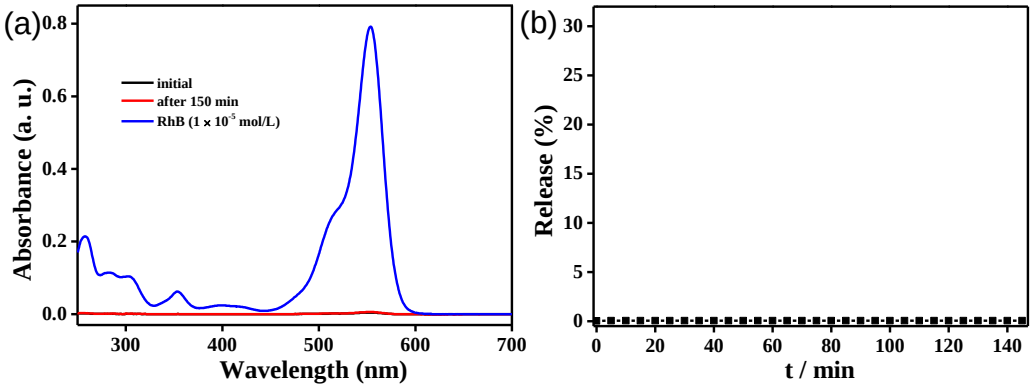

fig. S15. UV spectra (**a**) and release profile (**b**) of mechanized UiO-68-azo after addition of ethanol. Condition: ~3.7 mg UiO-68-azo, 3 mL deionized water, 30 µL ethanol.

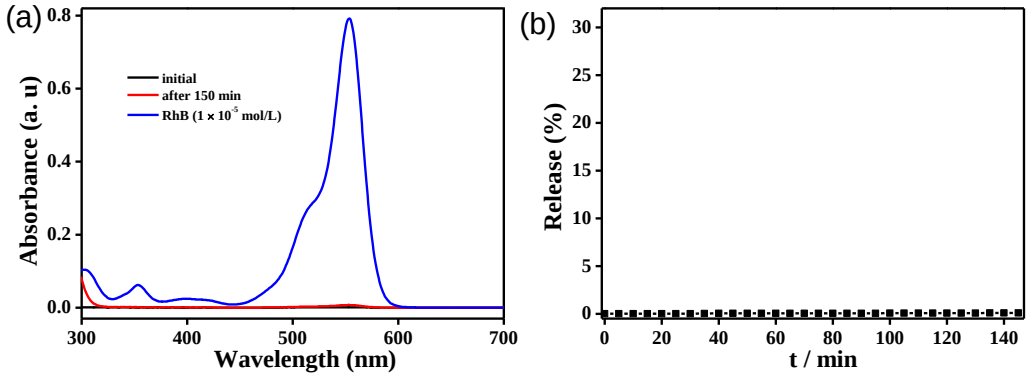

fig. S16. UV spectra (**a**) and release profile (**b**) of mechanized UiO-68-azo after addition of acetone. Condition: ~3.0 mg UiO-68-azo, 3 mL deionized water, 30 µL acetone.

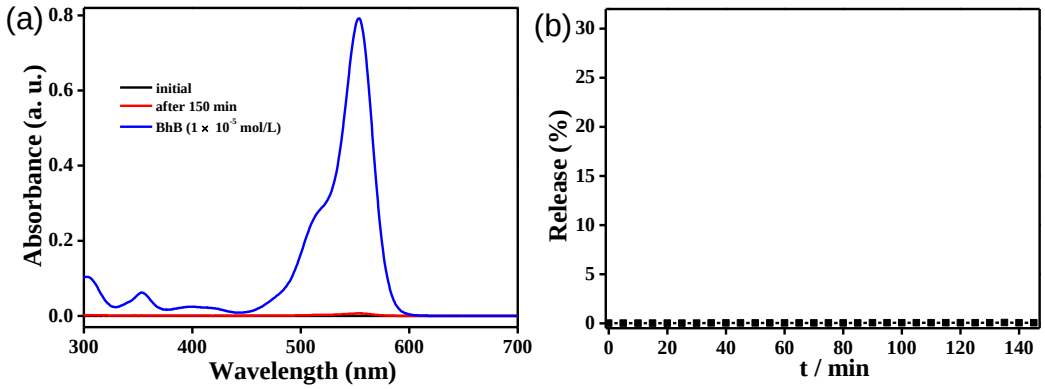

fig. S17. UV spectra (**a**) and release profile (**b**) of mechanized UiO-68-azo after addition of DMSO. Condition: ~3.3 mg UiO-68-azo, 3 mL deionized water, 30 μL DMSO.

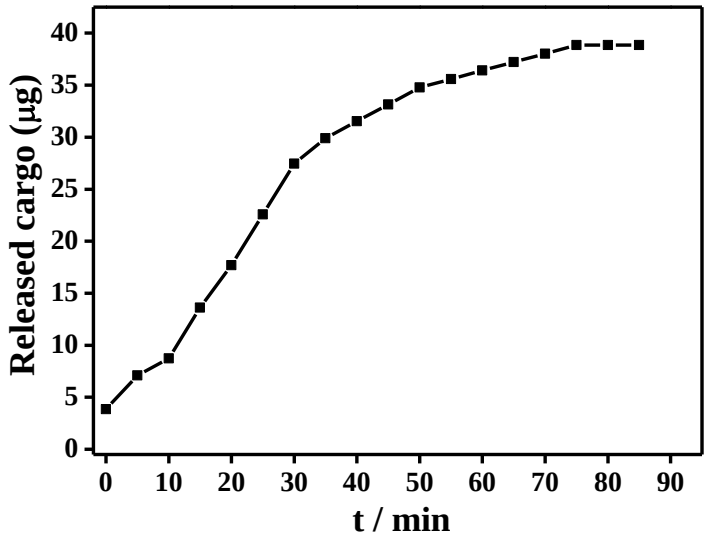

fig. S18. Release profile of uncapped RhB-loaded UiO-68-azo after UV irradiation. Condition: ~10.2 mg UiO-68-azo, 25 mL deionized water.

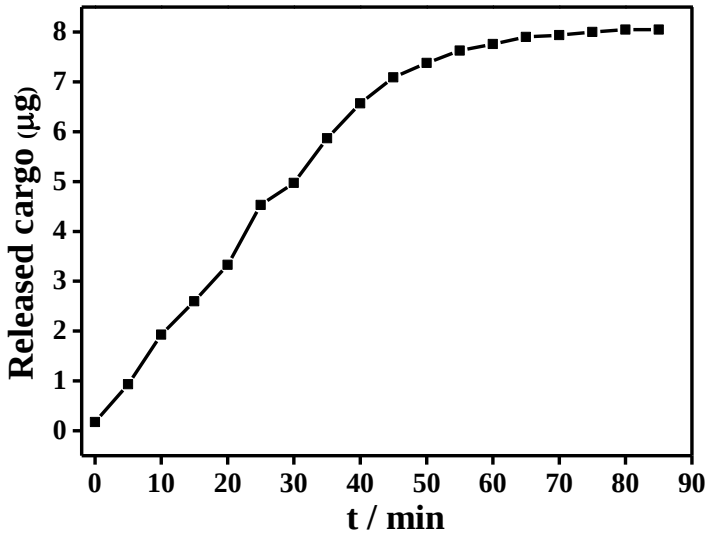

fig. S19. Release profile of uncapped RhB-loaded UiO-68-azo after addition of amantadine. Condition: ~2.2 mg UiO-68-azo, 3 mL deionized water, 0.24 mg amantadine.

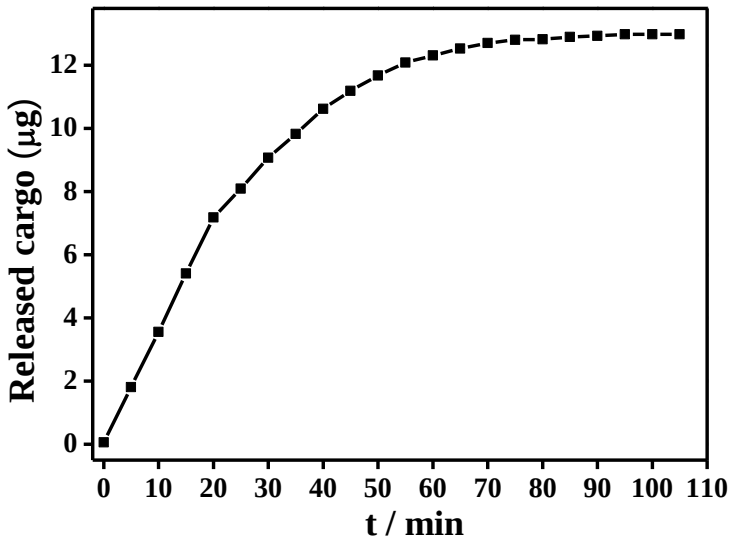

fig. S20. Release profile of uncapped RhB-loaded UiO-68-azo after addition of D-arabinose. Condition: ~3.2 mg UiO-68-azo, 3 mL deionized water, 1 mg D-arabinose.

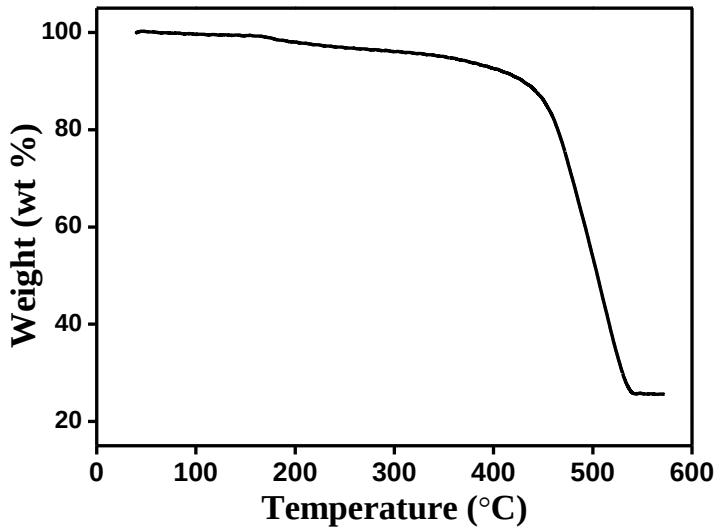

fig. S21. Thermogravimetric plot of UiO-68-azo.

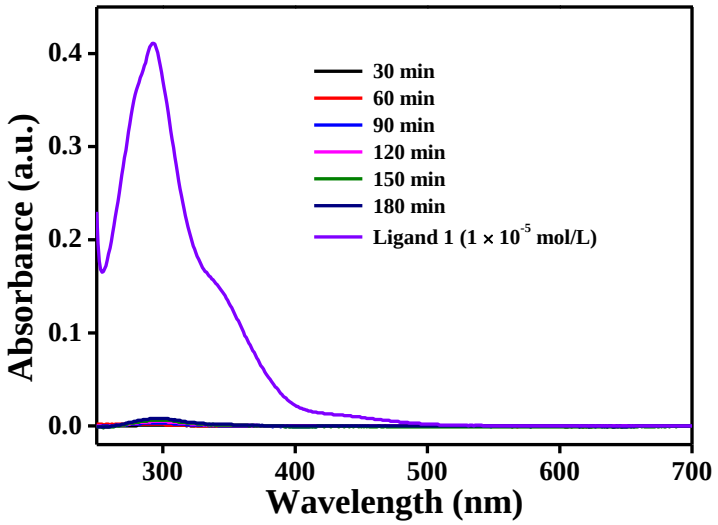

fig. S22. UV-visible spectra of Hepes buffer solution (pH=7.4) containing UiO-68-azo with different time. The purple line is the absorption curve of ligand **1** in a HEPES buffer solution (pH=7.4) with a concentration of 1×10^{-5} mol/L. Condition: ~ 9.0 mg UiO-68-azo, 3 mL HEPES buffer solution.

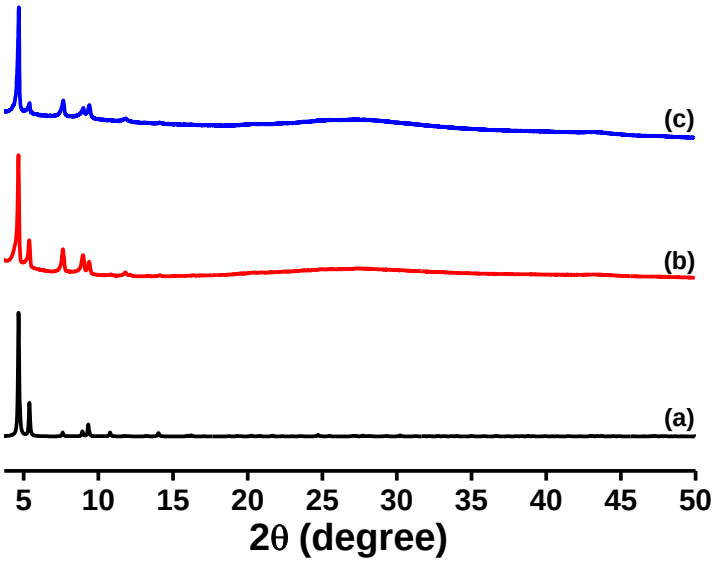

fig. S23. PXRD pattern of (**a**) simulated from the crystal structure of UiO-68-azo, (**b**) fresh UiO-68-azo, (**c**) after kept in a HEPES buffer solution for 3 h. The patterns were taken with crystals covered by a thin layer of water.

Experiments details

Release efficiency

In order to measure the amounts of RhB cargos after release, we recorded the absorption spectra of the solutions by a UV-Vis spectroscopy. The absorption band around 552 nm corresponds to the characteristic absorption peak of RhB cargo. The amounts of released RhB cargo were then calculated by using the extinction coefficients measured from standard RhB solutions of known concentrations.

Release study of RhB-loaded, β-CD capped UiO-68-azo after UV irradiation

In a typical experiment, RhB-loaded, β-CD capped UiO-68-azo was put in a viral and filled with 25 mL deionized water. The system was irradiated with UV lamp and the UV-vis spectra of solution were performed in every 5 min (fig. S9). Based on the standard RhB solutions of known concentrations, the release amount of RhB was calculated to be ~0.52 μmol. We then washed the crystal samples thoroughly until no red color was found. The rest RhB was collected and the total loading amount of RhB in mechanized UiO-68-azo was calculated to be ~0.96 μmol. The crystal was dried in the oven and the weight is ~8.6 mg. The release capacity is ~2.74 wt%.

Release study of RhB-loaded, β-CD capped UiO-68-azo after addition of amantadine and then UV irradiation

In a typical experiment, RhB-loaded, β-CD capped UiO-68-azo was put in a viral and filled with 25 mL deionized water. Amantadine (2 mg) was added to the solution and the UV-vis spectra of the solution were performed in every 5 min (fig. S11). Based on the standard RhB solutions of known concentrations, the release amount of RhB was calculated to be ~0.34 μmol. After that, the system was irradiated with UV lamp. The UV-vis spectra of the solution were again performed in every 5 min (fig. S11) and the release amount of RhB in this process were calculated to be ~0.06 μmol. We then washed the crystal samples thoroughly until no red color was found. The rest RhB cargos were collected and the total loading amount of RhB in mechanized UiO-68-azo was calculated to be ~0.70 μmol. The crystal was dried in the oven and the weight is ~6.3 mg. The release capacity is ~2.88 wt%.

Controlled Release study of RhB-loaded, *β*-CD capped UiO-68-azo

In order to further demonstrate amantadine-triggered release is caused by the dissociation of *β*-CD rings from the azobenezene stalks on the MOF surface, we have performed several controlled experiments, by adding other molecules (D-arabinose,

4-amino-1-naphthalenesulfonic acid sodium salt and sodium benzoate) or common solvents (ethanol, acetone and DMSO) as competitive agents. In a typical experiment, RhB-loaded, *β*-CD capped UiO-68-azo was put in a cuvette and filled with 3 mL deionized water. After adding these agents to the solution, the UV-vis spectra of the solution were measured in every 5 min. Based on the standard RhB solutions of known concentrations, the amount of RhB released was calculated. After that, the crystal samples were washed until no red color was found and the amount of the rest RhB was also calculated. The crystals were dried in the oven and also weighted.

After addition of these molecules (D-arabinose, 4-amino-1-naphthalenesulfonic acid sodium salt and sodium benzoate), a negligible release of RhB was detected (figs. S12-S14). According to the literature, each of these molecules has a lower binding constant with *β*-CD in aqueous solution than azobenzene and *β*-CD. As a result, their addition cannot efficiently trigger the dissociation of *β*-CD rings from the azobenzene stalks on the MOF surface and RhB cannot escape from the nanopores of mechanized UiO-68-azo. For adding common solvents (ethanol, acetone and DMSO), the UV-vis spectra of solutions over time also showed a negligible amount of RhB was released (figs. S15-S17). Therefore, the amantadine-triggered release is caused by the dissociation of *β*-CD rings from the azobenezene stalks on the MOF surface, which will open the gate to the nanopores and release the cargo.

Preparation of uncapped RhB-loaded UiO-68-azo

A fresh sample of UiO-68-azo (~ 40 mg) was immersed in 15 mL water solution containing Rhodamine B (15 mg mL^{-1}) for 12 h in the dark. After decanting the solution, the sample was washed with water for several times. Then, the sample was used directly for release study.

Release study of uncapped RhB-loaded UiO-68-azo

In order to demonstrate that the supramolecular complex on the surface is playing a central role for holding the cargo within UiO-68-azo, we have performed several control experiments: 1) release behavior of uncapped RhB-loaded UiO-68-azo; 2) release behavior of uncapped RhB-loaded UiO-68-azo after UV irradiation; 3) release behavior of uncapped RhB-loaded UiO-68-azo after addition of amantadine or D-arabinose. In every experiment, the UV-vis spectra of the solutions were measured every 5 min. Based on the standard RhB solutions of known concentrations, the amount of RhB released was calculated. After that, the crystal samples were washed until no red color was found and the amount of the rest RhB was calculated. The

crystals were dried in the oven and then weighted.

From these experiments, we have several conclusions: (1) for the uncapped RhB-loaded UiO-68-azo, the RhB can be spontaneously released from the nanopores of UiO-68-azo, indicating again the importance of the supramolecular *β*-CD⊂azobenzene complex on the MOF surface; (2) the encapsulation efficiency of uncapped RhB-loaded UiO-68-azo was significantly lower than that of *β*-CD capped UiO-68-azo, which can be ascribed to the loss of RhB molecules from the interiors in the progress of washing and centrifuge.

Stability of UiO-68-azo in a buffer solution

We studied the stability of UiO-68-azo in a HEPES buffer solution (pH=7.4). After adding UiO-68-azo (~9.0 mg) into a HEPES buffer solution (3 mL), the UV-vis spectra of the solution were measured every 30 min (fig. S22). Based on the standard solutions of ligand **1**, a very small amount of ligand **1** (~0.7 nmol) was detected after leaving UiO-68-azo in a buffer solution for 3 hours. This is reasonable, since the ligands or metals on the exterior surface of UiO-68-azo are in unsaturated coordination and may dissociate when kept in a solvent. However, based on the weight of UiO-68-azo, the ratio of dissociated ligand is extremely slow (~0.004%), indicating that the dissolution of UiO-68-azo is very slow at a physiologically relevant pH. In addition, from PXRD experiments, the framework is retained in the buffer solution.

Nitrogen absorption study of UiO-68-azo before and after UV irradiation

The nitrogen adsorption and desorption isotherms of UiO-68-azo were performed at 77 K. After that, the samples were exposed under UV irradiation for 3 h and then their adsorption and desorption isotherms were measured. Before the measurement, approximately 30 mg of activated UiO-68-azo were degassed in vacuum at room temperature for 18 h. The isotherm points chosen to calculate the BET surface area were subject to the three consistency criteria detailed by Walton and Snurr.

Digestion of UiO-68-azo

For UiO-68-azo digestion, approximately 10 mg activated samples were digested with sonication in 1 mL DMSO and 10 μL 30% HF aqueous solution. After that, water was added to the resulting solution until no further precipitate was detected. The precipitate was collected by filtration, washed with water and dried in vacuum.

Crystal Data Collection for UiO-68-azo

Suitable crystals of UiO-68-azo were mounted on nylon loops. The single-crystal x-ray diffraction data was collected at 100 K at the Beijing Synchrotron Radiation Facility, beam line station 3W1A equipped with a MarCCD-165 detector (the monochrome X-ray source is produced by an accelerator and selected by a double crystal monochromator, $\lambda = 0.8000$Å). Scattering factors for the wavelength of 0.800 Å for use in SHELXL-2014 were calculated for all elements using the program XDISP and were implemented in SHELXL-2014 using DISP commands. Structures were solved by direct methods in SHELXT-2014 and refined by full-matrix least-squares on F^2 using SHELXL-2014. The Zr-bridging oxo and hydroxo ions are disordered with each other and were refined with a 1:1 ratio. No restraints were applied for positions or ADPs. Ligand O and C atoms were subjected to a rigid bond restraint (RIGU in Shelxl). All C-C bond distances within aromatic rings were restraint to be similar to each other. The central benzene ring is 1:1 disordered over two symmetry equivalent positions. The functional substituents at the central benzene ring are disordered over eight equivalent positions and subject to large thermal libration and disorder. They were not resolved in the electron map and have been omitted from the structural model. The sum formula given is for the actual compound including the substituents, but ignoring unresolved solvate molecules. Residual electron density from disordered substituents and from disordered solvate molecules was corrected for using reverse Fourier transform methods as implemented in the SQUEEZE routine in the program Platon. Crystal data and structure determination summary for UiO-68-azo are listed in Table S1.

Simulation details

As mentioned above, due to the severe disorder of the azobenzene groups in the crystal structure of UiO-68-azo, we cannot locate their position in the crystal structure. As such, we simulated the hypothetical crystal structures of *trans*-UiO-68-azo using the Material Studio software package. The crystal structure of *trans*-UiO-68-azo with reduced crystal symmetry for avoiding disorder was used as a starting model. Azobenzene groups were generated and optimized using the forcite geometry optimization tool, implemented in Material Studio. During the optimization procedure, the unit cell parameters and Zr_6 cluster units were kept rigid. The universal force field was used for the geometric optimization of the obtained structure. Accordingly, we also simulated the hypothetical crystal structures of *cis*-UiO-68-azo.

From the simulated crystal structures and by using SOLV procedure of the PLATON software with a probe radius of 1.8 Å, the calculated solvent-accessible void volumes for *trans*-UiO-68-azo and *cis*-UiO-68-azo were shown to be very close. Since they have same net topology and very close solvent-accessible void volumes, the adsorption behavior of nitrogen before and after UV irradiation should be very similar.

Staring from the simulated crystal structure, we have also compared the size of RhB guest and the aperture of the triangle window of the simulated *trans*-UiO-68-azo (fig. S8). Indeed, the diffusion of RhB molecules through some triangle windows is forbidden in some directions, due to the blocking by azobenzene unit. However, the RhB molecules are supposed to pass through these triangle windows and then diffuse into the pore from where they can move on. In addition, some triangle windows have no blocking azobenzene units, which can also allow the RhB molecules to enter the crystal pores.Therefore, after immersing UiO-68-azo in an RhB aqueous solution, the RhB molecules can diffuse into the framework.